International Journal of Environmental Sciences
ISSN: 2229-7359
Vol. 11 No. 6s, 2025
https://www.theaspd.com/ijes.php

Computational ADMET, Drug-Likeness, QSPR and Molecular Docking Analysis of Phytochemicals from *Avicennia marina*

Shital S Chavan[1], Prashant B Shamkuwar[1], Manoj G Damale[2]
[1]Department of Pharmacognosy, Government college of Pharmacy, Chhatrapati Sambhajinagar, M.S., India.
[2]Department of Pharmaceutical Chemistry, Srinath College of Pharmacy, Chhatrapati Sambhajinagar, M.S., India.
Corresponding Author
Ms. Shital S Chavan
Government college of Pharmacy, Chhatrapati Sambhajinagar, M.S., India.Shitalchavan28@ymail.com

Abstract
The growing demand for novel therapeutics with multi-target efficacy and minimal toxicity has accelerated the exploration of plant-derived bioactive compounds using computational approaches. Avicennia marina, a mangrove species known for its traditional medicinal use, was investigated in this study for its pharmacological potential through a comprehensive in silico approach. Phytochemicals present in the hydroalcoholic leaf extract were subjected to pharmacokinetic (ADME), drug-likeness, toxicity, Quantitative Structure–Property Relationship and molecular docking analyses to evaluate their suitability as drug candidates. ADMET profiles were predicted using the pkCSM server, while toxicity parameters, including LD_{50}, organ toxicity, and cytochrome P450 inhibition, were evaluated via the ProTox-III platform. Drug-likeness was assessed according to Lipinski's Rule of Five using Chemsketch 2019.2, indicating that most compounds complied with the criteria for oral bioavailability. A Quantitative Structure–Property Relationship (QSPR) study was performed using a wide array of 2D and 3D molecular descriptors, establishing correlations between physicochemical properties and molecular structures with the aid of SPSS software. Molecular docking was conducted using AutoDock Vina against selected protein targets—DNA gyrase, sterol 14-alpha demethylase (CYP51), main protease (Mpro), and catalase—to evaluate binding affinity and inhibitory potential. The study revealed that several phytochemicals, including 4-(4-Hydroxyphenyl)-2-butanone, O-[2-galloyl-6-p-coumaroylglucoside], Catechin 3',5-diglucoside, and Paromamine, exhibited favorable ADMET profiles, strong binding affinities, and significant drug-likeness. These findings highlight the therapeutic potential of Avicennia marina phytoconstituents as promising leads for antibacterial, antifungal, antiviral (anti-COVID-19), and antioxidant drug development, warranting further experimental validation.

Key Words: *Avicennia marina, Absorption, Distribution, Metabolism, Excretion, Toxicity, Quantitative Structure–Property Relationship, Molecular docking, antibacterial, antifungal, antiviral (anti-COVID-19) antioxidant*

INTRODUCTION

The global burden of infectious diseases, antibiotic resistance, and emerging viral outbreaks has intensified the need for novel therapeutic agents with multi-target potential and minimal toxicity(Muteeb et al., 2023). Over the past decades, natural products derived from medicinal plants have proven to be a valuable source of structurally diverse and pharmacologically active compounds(Chaachouay & Zidane, 2024). Among these, mangrove species have attracted growing interest due to their unique ability to thrive in extreme environments, often leading to the biosynthesis of potent secondary metabolites(Basyuni et al., 2019). One such species is *Avicennia marina* (grey mangrove), a halophytic plant widely distributed in coastal regions and traditionally used in folk medicine for treating various ailments including wounds, infections, inflammation, and oxidative stress-related disorders(Wu et al., 2023). Despite the ethnopharmacological relevance of *Avicennia marina*, its phytochemical constituents and their potential roles as drug candidates remain underexplored through modern scientific approaches. The integration of computational and predictive methodologies in drug discovery has revolutionized early-phase screening, allowing researchers to evaluate the

pharmacokinetic behavior, toxicity risks, and molecular interactions of compounds with therapeutic targets without the need for extensive laboratory testing(Agamah et al., 2020). These in silico techniques provide a cost-effective and time-efficient alternative for identifying promising lead compounds, guiding subsequent in vitro and in vivo validations(Naithani & Guleria, 2024). In this context, the present study focuses on the hydroalcoholic extract of *Avicennia marina* leaves, aiming to investigate the pharmacokinetic, toxicological, drug-likeness, and molecular interaction profiles of its phytochemicals through a comprehensive in silico framework(Mirazi et al., 2016). The Absorption, Distribution, Metabolism, Excretion, and Toxicity (ADMET) characteristics of the selected compounds were predicted using the pkCSM server, while toxicity endpoints such as LD_{50}, organ toxicity, and cytochrome P450 inhibition were evaluated through the ProTox-III platform(Banerjee et al., 2024; Pires et al., 2015). These predictions are crucial for assessing the safety and bioavailability of candidate molecules during the early stages of drug development. To further assess the oral bioactivity potential of the compounds, Lipinski's Rule of Five (LRO5) was employed. This widely accepted rule considers critical physicochemical properties such as molecular weight, lipophilicity (LogP), hydrogen bond donors and acceptors, and topological polar surface area—factors that influence drug absorption and permeability(Doak & Kihlberg, 2017). Physicochemical parameters were calculated using Chemsketch software, providing a foundation for drug-likeness evaluation.In addition, a Quantitative Structure–Property Relationship (QSPR) analysis was performed to establish meaningful relationships between the molecular structure of the phytochemicals and their predicted biological or physicochemical properties(Van Den Maagdenberg et al., 2024). Various 2D and 3D descriptors—such as molecular volume, surface area, dipole moment, HOMO-LUMO energies, and shape indices—were computed, and statistical correlation models were constructed using SPSS software(De Lile et al., 2020). These insights not only highlight the key molecular determinants of bioactivity but also provide predictive tools for rational drug design. Finally, the study incorporated molecular docking simulations to evaluate the binding affinity of selected phytochemicals against biologically relevant protein targets, including DNA gyrase (bacterial target), sterol 14-alpha demethylase (antifungal target), main protease (Mpro, a target in SARS-CoV-2), and catalase (antioxidant target)(Anwar et al., 2024; Collin et al., 2011; Jin et al., 2020; Monk et al., 2020). Using AutoDock Vina and Discovery Studio, the interactions between the ligands and the active sites of the proteins were visualized and analyzed, enabling the identification of strong binders with potential therapeutic efficacy(Agu et al., 2023). This integrative computational investigation not only highlights the drug-likeness and pharmacokinetic viability of *Avicennia marina* phytochemicals but also identifies lead compounds with potent antibacterial, antifungal, antiviral, and antioxidant properties. Among the screened compounds, 4-(4-Hydroxyphenyl)-2-butanone, O-[2-galloyl-6-p-coumaroylglucoside], Catechin 3',5-diglucoside, and Paromamine emerged as particularly promising candidates. These findings underscore the potential of *Avicennia marina* as a reservoir of bioactive compounds and provide a valuable foundation for future pharmacological and clinical research in the development of novel therapeutic agents(ElDohaji et al., 2020).

MATERIAL AND METHODS

Insilico ADMET Predictions:

Forecasting the Absorption, distribution, metabolism and elimination properties of chemical constituents is a crucial and rate-limiting step in the drug discovery process .In this study, prediction of pharmacokinetic and toxicity profiles performed using the PKCMS online server (https://biosig.lab.uq.edu.au/pkcsm/prediction)(Kauthale et al., 2017). Prediction of toxicity of chemical server Protox III (https://tox.charite.de/protox3/index.php?site) used to predict the toxicity of chemical compounds. Prediction of toxicity chemical are categories depends upon toxicity dose(lethal dose) LD_{50} . It also predicts Organ Toxicity and CYP substrate inhibitor in the metabolism prediction(Arulanandam et al., 2022) .

Prediction of Druglikness (LRO5)

Determination and analysis of druglikeness of chemical constituents or new chemical entities is important process in drug discovery. Christopher A. Lipinski in 1997 formulated some important observation regarding for orally active drugs like molecular weight (≤ 500 Dalton), LogP value (≤ 5.5), TPSA (≤ 140 Å), n-HBD (≤ 5), n-HBA (≤ 10). The molecules follows the above ranges for physicochemical properties have very good oral activity(Benet et al., 2016). The physicochemical parameters were predicted by the Chemsketch 2019.2 software.

Quantitative Structure Property Relationship:

The aim of Quantitative Structure Property relationship study is to establish the quantitative relationship between physicochemical parameter and structure of bioactive conformation. Physicochemical properties of the molecules like electronic, steric, Lipophlicare calculated in the form of 2D and 3D descriptor properties such as Molecular Weight, Number of Atoms, Number of Bonds, Number of Hydrogen Bond Donors, Number of Hydrogen Bond Acceptors, Number of Aromatic Rings, Number of Rotatable Bonds, Number of Nitrogen, Oxygen, and Sulphur Atoms,Wiener Index, Randic Index, Kier Shape Indices,LogP, Topological Polar Surface Area, Molar Refractivity, Surface Area and Volume, Molecular Volume, Surface Area, Shape Indices, Inertia Tensor Eigenvalues, Dipole Moment, HOMO–LUMO Energies, Partial Atomic Charges,etc. The Lipophlic descriptors are designated and calculated as LogP and LogS whereas electronic descriptors or quantum chemical descriptors are represented as Total Energy E_{TOT},Energy of Highest Unoccupied Molecular Orbital E_{HOMO}, and Energy of Lowest Unoccupied Molecular Orbital E_{LUMO}. Steric nature of the molecules is calculated as molecular weight and molecular volume(Katritzky et al., 2010). The Total clearance of the drug is predicted in the form of CL_{TOT} using online pkCSM server (https://biosig.lab.uq.edu.au/pkcsm/). The Quantitative Property relationship between Properties and structure is build by Statistical Package for the Social Sciences (SPSS) statistical tool version 28.(Nainggolan et al., 2025)

MOLECULAR DOCKING:

Preparation of Three dimensional X-ray crystal Structure of Target Protein:

Molecular docking study functions as a method for assessing the binding affinity and inhibitory potential of Phytochemicals against the X-ray crystal structure of various target proteins like DNA gyrase, sterol 14-alpha demethylase (CYP51),main protease and catalase (Hargrove et al., 2017; Jin et al., 2020; Kumara et al., 2021; Lafitte et al., 2002; Lu et al., 2014). AutoDock Tools 1.5.4 (ADT) was used to create the input files for docking. Water molecules and heteroatoms were removed from the protein structure, polar hydrogen atoms were added, and partial atomic charges were given via the Kollman unified charge technique(Allouche, 2011).For every phytochemical, non-polar hydrogen's were consolidated, Gasteiger partial charges were assigned, and rotatable bonds were specified. The protein structure was then stored in the AutoDock PDBQT file format. A grid box was centered on the active site of target proteins where the co-crystallized Phytochemical resided, and the dimensions were established to examine the interactions between the Phytochemical and the protein(Akolkar et al., 2020). Default settings were used for Vina docking. The two-dimensional and three-dimensional molecular interactions between the synthesized derivatives and the protein were examined and visualized with Discovery Studio Visualiser V21.1.0.20298(Trott & Olson, 2010).

Preparation of Three dimensional structures of Phytochemical Molecules

The three dimensional structure of phytochemicals molecules were downloaded from pubchem(https://pubchem.ncbi.nlm.nih.gov/). The Chemsktech Freeware 14.01 (Advanced Chemistry Development) was used to optimize geometry and energy usingMerck molecular force field (MMFF94). The Optimize forms are stored in .MOL2 format(Hwang et al., 2020).

International Journal of Environmental Sciences
ISSN: 2229-7359
Vol. 11 No. 6s, 2025
https://www.theaspd.com/ijes.php

RESULTS AND DISCUSSION:

Insilico ADMET Predictions:

Pharmacokinetic profile of the Paroramine, Catechin 3,5-diglucoside, 4-(4-Hydroxyphenyl)-2 butanone O-[2-galloyl-6-pcoumaroylglucoside], Maltoheptaose,5-methyl-2-pentylthiazole,diphenylamine,Leptophos has represented in Table1.The predicted absorption parameter such as water solubility in the range of -2.16 log mol/l to -2.03 log mol/l suggest the phytochemicals have moderate solubility and dissolution property . The intestinal permeability is predicted by Caco2 Permeability indicates all them have very good passive absorption potential. Similar results are corresponded in the percent Intestinal absorption ranges from 84.87% to 55.81%. The skin permeability values also indicates they good permeation between -3.40 log Kp to -3.43 log Kp. None of the Phytochemical compound acting substrate or inhibitors for the P-glycoprotein suggesting minimal efflux.Volume of distribution is indicating distribution of the drug in the systemic circulation where it ranges from 1.23 to 0.14 suggest they have moderate volume of distribution. Fraction unbound(Fu) indicates moderate to high indicates maximum amount of compounds are available for the exerting pharmacological action.BBB permeability indicates maximum number of Phytochemical except 5-methyl-2-pentylthiazole does not have good BBB permeability and mostly excluded from the Blood Brain Barrier.The interaction with metabolic enzymes are predicted by substrate prediction with common cytochrome P450 isoenzymes suggest they rarely interacting with CYPs. Total clearance rates were generally low, ranging from 0.25 to 0.65 log ml/min/kg. Paroramine showed the highest clearance rate, suggesting quicker systemic elimination, whereas Leptophos showed the slowest. None of the compounds were renal OCT2 substrates, indicating likely hepatic or alternative routes of elimination. None of the compounds exhibited AMES toxicity, hERG inhibition, hepatotoxicity, or skin sensitization, indicating a favorable toxicological profile. The maximum tolerated dose (MTD) was comparable across all compounds (log mg/kg/day around 0.43–0.53).Acute oral toxicity in rats was in a narrow range (2.33–2.45 mol/kg), suggesting moderate toxicity levels. Predicted toxicity class ranged from Class 3 to Class 5, with Maltoheptaose having the highest predicted toxicity (Class 3), while Catechin, Diphenylamine, and others were placed in Class 5, indicating relatively lower acute toxicity. Prediction accuracy values for the toxicity models were consistent across compounds (70–74%), reflecting acceptable reliability of the computational predictions. Toxicity radar highlights the toxicity predictions are shown in the figure of 4-(4-Hydroxyphenyl)-2 butanone O-[2-galloyl-6-pcoumaroylglucoside], Catechin 3',5-diglucosideand Paromamineas shown in figure 1.

Table 1. ADMET property predictions of Phytochemicals

Property Prediction	Paroramine	Catechin 3,5-diglucoside	4-(4-Hydroxyphenyl)-2 butanone O-[2-galloyl-6-pcoumaroylglucoside]	Maltoheptaose	5-methyl-2-pentylthiazole	Diphenylamine	Leptophos
Absorption							
Water Solubility (log mol/l)	-2.14	-2.08	-2.37	-2.13	-2.16	-2.03	-2.09
Caco2 Permeability (log Papp in 10–6 cm/s)	3.02	3.80	3.10	2.24	2.90	3.38	1.32

Intestinal absorption (% Absorbed)	66.30	71.50	83.90	62.38	80.31	84.87	55.81
Skin permeability (log Kp)	-3.43	-3.40	-3.40	-3.43	-3.40	-3.40	-3.40
P-glycoprotein substrate (Yes/No)	No	No	No	No	No	No	No
P-glycoprotein I Inhibitor (Yes/No)	No	No	No	No	No	No	No
Distribution							
Volume of Distribution (log L/kg)	0.56	0.49	1.23	0.67	0.73	0.14	0.54
Fraction Unbound (Fu)	0.45	0.89	0.54	0.56	0.23	0.89	0.56
BBB permeability (log BB)	-0.45	-0.56	-0.56	-0.60	1.65	0.80	-0.56
Metabolism							
CYP2D6 Substrate(Yes/ No)	No	No	No	No	No	No	No
CYP3A4 Substrate(Yes/ No)	No	No	No	No	No	No	No
CYP1A2 Substrate(Yes/ No)	No	No	No	Yes	No	No	No
CYP2C19 (Yes/No)Substrate	No	No	No	No	No	No	No
CYP2C9 Substrate(Yes/ No)	No	Yes	No	No	No	No	No
CYP2D6 Substrate(Yes/ No)	No	No	No	No	No	Yes	No
CYP3A4 Substrate(Yes/ No)	No	No	No	No	No	No	No
Excretion							

International Journal of Environmental Sciences
ISSN: 2229-7359
Vol. 11 No. 6s, 2025
https://www.theaspd.com/ijes.php

Total clearance(log ml/min/kg)	0.65	0.45	0.62	0.43	0.54	0.45	0.25
Renal OCT2 substrate (Yes/No)	No	No	No	No	No	No	No
Toxicity							
AMES toxicity (Yes/No)	No	No	No	No	No	No	No
Max Tol Dose (log mg/kg/day)	0.43	0.45	0.44	0.44	0.43	0.45	0.53
hERG inhibitor (Yes/No)	No	No	No	No	No	No	No
Oral rat acute toxicity (mol/kg)	2.43	2.43	2.33	2.45	2.43	2.34	2.43
Hepatotoxicity (Yes/No)	No	No	No	No	No	No	No
Skin sensitization (Yes/No)	No	No	No	No	No	No	No
Predicted toxicity class	Class 4	Class 5	Class 5	Class 3	Class 4	Class 5	Class 5
Prediction accuracy(%)	70.67	71.65	71.89	71.87	71.45	71.45	73.84

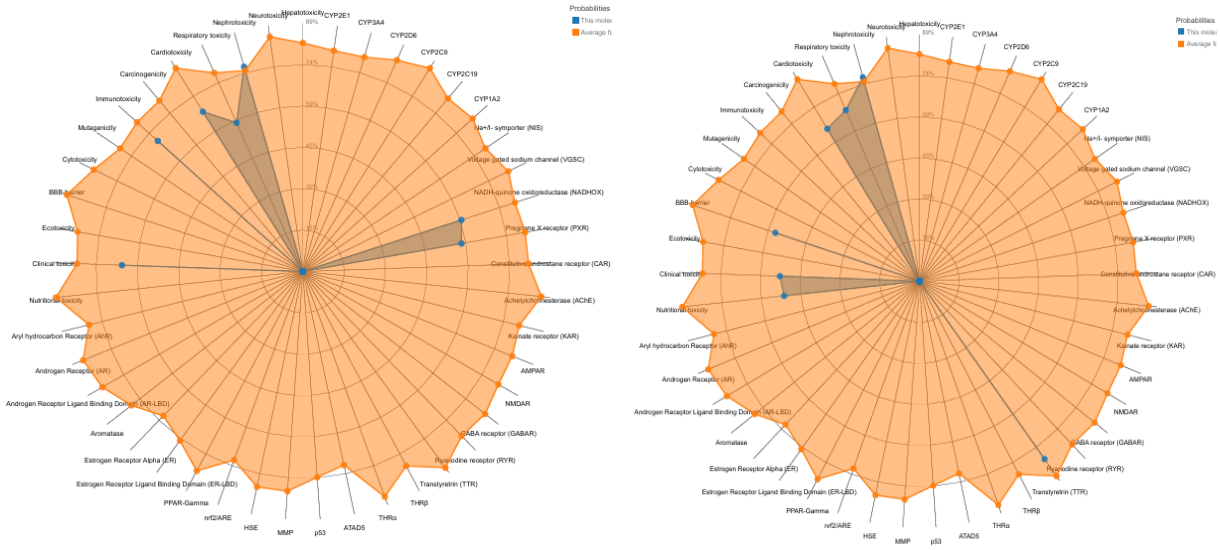

International Journal of Environmental Sciences
ISSN: 2229-7359
Vol. 11 No. 6s, 2025
https://www.theaspd.com/ijes.php

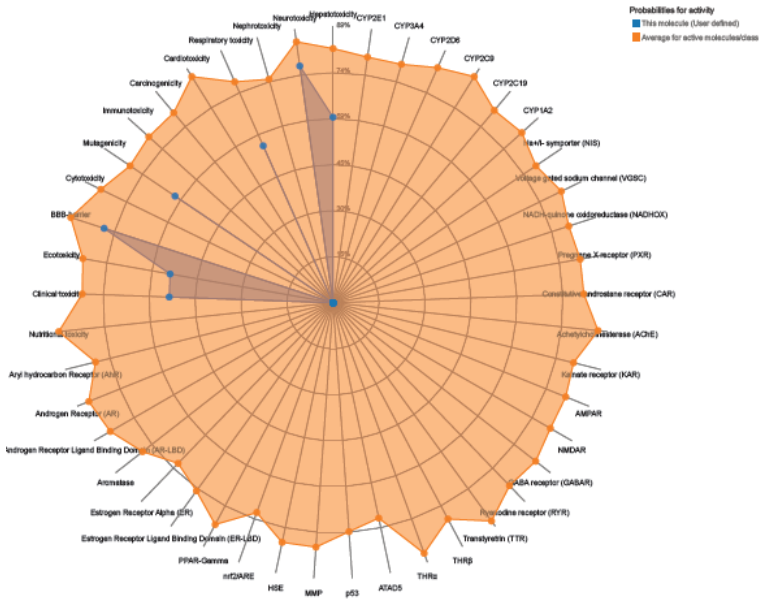

Figure 1Toxicity radar of 4-(4-Hydroxyphenyl)-2 butanone O-[2-galloyl-6-pcoumaroylglucoside], Catechin 3,5-diglucoside,Paroramine

Prediction of Druglikness (LRO5):

The prediction of druglikness based on lipski rule of five suggests that molecular weight of Paroramine, 5-methyl-2-pentylthiazole, Diphenylamine and Leptophos follows in the accepted level. Whereas Catechin 3,5-diglucoside, 4-(4-Hydroxyphenyl)-2 butanone O-[2-galloyl-6-pcoumaroylglucoside] and Maltoheptaose violating the LRO5 for molecular weight. Prediction of partition coefficient LogP value suggest that all the them polar and nonpolar properties. The polar solubility is calculated by TPSA which suggest that Catechin 3,5-diglucoside, Catechin 3,5-diglucoside, 4-(4-Hydroxyphenyl)-2 butanone O-[2-galloyl-6-pcoumaroylglucoside] and Maltoheptaose does not follows in acceptable range. Prediction of Number of hydrogen bond donor and acceptor suggest that Paroramine, 5-methyl-2-pentylthiazole, Diphenylamine and Leptophos follows in the accepted level as given in table 2.

Table 2. Prediction values of Druglikness as per RO5

Property Prediction	Paroramine	Catechin 3,5-diglucoside	4-(4-Hydroxyphenyl)-2 butanone O-[2-galloyl-6-pcoumaroylglucoside]	Maltoheptaose	5-methyl-2-pentylthiazole	Diphenylamine	Leptophos
Molecular Weight≥500	372	514	638	1153	169	16	16
LogP≥5	5	3.51	2.87	-16.00	3.18	1.00	1.00

NHBD≥5	0	7	7	36	1	0	0
NHBA≥10	2	10	10	23	0	1	1
TPSA≥150	120	268	200	585	41.13	10	10

3.3 Development of Quantitative Structure Property Relationship Models:

The Seven QSPR models developed among them best fitted QSPR model were chosen based on regression statisticsfrom the equation computed. The following equation is found best

$$\text{CLtotal} = \frac{1}{0.262\ \text{ELUMO} + 3.012}$$

Where n=5, R= 0.923, SE = 0.075, F = 94.22, Sig = 0.001

The above equation highlights best correlation coefficient whichis denoted by R = 0.923, which least significance Sig = 0.001 and standard error SE = 0.075 and significantly higher F value = 94.22. Physicochemical parameter which determines the total clearance (CLtotal) is electronic descriptor E_{LUMO} given in table3 and table 4.

Table 3: QSPR relationship of physicochemical properties to 1/CLtotal

Property (Independent variable)	**R**	**SE**	**F**	**Sig**	**Equation**
LogP	0.912	0.213	30.02	0.001	CLtotal = 1/0.260 LogP+ 2.904
LogS	0.915	0.236	30.48	0.001	CLtotal = 1/0.284LogS+ 2.936
Etotal	0.875	0.326	32.43	0.002	CLtotal = 1/0.247Etotal+ 1.476
EHOMO	0.901	0.216	30.25	0.001	CLtotal = 1/0.271E_{HOMO} + 1.301
ELUMO	0.923	0.262	94.22	0.001	CLtotal = 1/0.262 E_{LUMO} + 3.012
MW	0.874	0.325	32.45	0.001	CLtotal = 1/0.245MW+ 1.406
MR	0912	0.213	30.02	0.001	CLtotal = 1/0.260 MR+ 2.904

Table 4 Predicted data of physicochemical properties of phytochemicals

Compound Name	Lipophilic		Electronic			Steric		CLtotal	Log(1/CLtotal)
	Log P	LogS	Etotal	E_{HOMO}	E_{LUMO}	MW	MR		

Paroramine	5.0	-1.96	37.23	-11.23	-8.51	372	73.23	0.41	0.38
Catechin 3,5-diglucoside	3.15	-2.30	39.56	-12.53	-8.35	514	87.51	0.47	0.41
4-(4-Hydroxyphenyl)-2 butanone O-[2-galloyl-6-pcoumaroylglucoside]	2.87	-2.03	38.45	-11.46	-8.23	638	110.23	0.43	0.46
Maltoheptaose	-16.00	-2.23	40.23	-12.23	-8.14	1153	86.36	0.46	0.47
5-methyl-2-pentylthiazole	3.18	-2.34	41.23	-11.36	-8.23	169	84.23	0.40	0.23
Diphenylamine	1.0	-2.89	39.42	-11.85	-8.75	16	56.42	0.48	0.45
Leptophos	1.0	-2.81	39.23	-11.80	-8.63	16	55.23	0.40	0.46

LogP: Partition coefficient, LogS: Solubility, Etotal: Minimum energy (kcal/mol), EHOMO: Highest occupied molecular orbital (eV), ELUMO: Lowest unoccupied molecular orbital (eV), MW: Molecular weight (g/mol), MR: Molar refractivity (cm3/mol), CLtotal: Clearance total (log ml/minute/kg).

MOLECULAR DOCKING

The inhibitory potentials of Phytochemicals were examined by molecular docking studies using the crystal structure of various target proteins such as DNA gyrase, sterol 14-alpha demethylase (CYP51), main protease and catalase to elucidate the binding energy, binding affinity, binding mechanism, and molecular interactions. The table 5 represents a summary of the docking scores, interacting residues, and kinds of interactions of phytochemicals.

Table 5 Molecular docking details of Phytochemicals against selected drug targets

Sr. No	**Name of Compound**	**Docking Score(Kcal /Mol) PDB ID:5TZ1**	**Docking Score(Kcal /Mol) PDB ID:6LU7**	**Docking Score(Kcal /Mol) PDB ID:1KZN**	**Docking Score(Kcal /Mol) PDB ID:4URN**	**Docking Score(Kcal /Mol) PDB ID:2CAG**
1	Paromamine	-4.6609	-7.5971	-5.4654	-7.5505	-2.2878
2	Catechin 3',5-diglucoside	-5.5553	-3.1349	-5.5792	-7.9564	-5.4516
3	4-(4-Hydroxyphenyl)-2 butanone O-[2-galloyl-6-pcoumaroylglucoside]	-8.2362	-2.2395	-8.1188	-11.704	-4.8993
4	Maltoheptaose	-4.2726	-1.0521	-2.6457	-7.2885	-1.6203
5	5-methyl-2-pentylthiazole	-3.5405	-1.4683	-4.535	-3.587	-2.1784
6	diphenylamine	-3.703	-2.4336	-3.126	-3.1873	-2.002

7	Fenoprop	-2.3257	-0.3076	-3.2792	-3.7152	-2.0873
8	(±)-Leptophos	-3.3326	-0.6983	-4.1602	-3.1071	-2.1398

The antifungal potential of Phytochemical is evaluated by molecular docking studies using the crystal structure of sterol 14-alpha demethylase (CYP51) from C. *albicans* (PDB ID: 5TZ1). The molecular docking study suggest that 4-(4-Hydroxyphenyl)-2 butanone O-[2-galloyl-6-pcoumaroylglucoside], Catechin 3',5-diglucosideand Paromamine have highest inhibitory potential indicated by docking score -8.2362 Kcal/Mol, -5.5553 Kcal/Mol and -4.6609 Kcal/Mol respectivelyamong the all the phytochemicals.

The 4-(4-Hydroxyphenyl)-2 butanone O-[2-galloyl-6-pcoumaroylglucoside]shown high binding energy -8.2362Kcal/Mol.Polar amino acid TYR132 interact with hydroxyl group hydrogen atom of terminal phenyl ring with conventional hydrogen bond interactions with distance of 1.92 Å. Nonpolar amino acid residues ILE304 and CYS470 interact with hydroxyl hydrogen's of glucose unit by forming conventional hydrogen bond interactions with distance of 2.07 and 2.61 Å respectively. Nonpolar amino acid residues LEU376 and PRO462 interacts with galloyl unit hydroxyl hydrogen atoms by conventional hydrogen bond interactions with distance of 1.93 and 1.89 Å respectively. Nonpolar amino acid GLY303 and PRO375 also interact with hydrogen atom and oxygen atom of hydroxyl group by forming carbon hydrogen bond interactions 2.69 and 2.59 Å respectively. Binding site amino acid residue such as LEU139, LYS143, LEU376 and PHE463 interacts with Pi lone and alkyl interactions with various distances as shown in figure 2

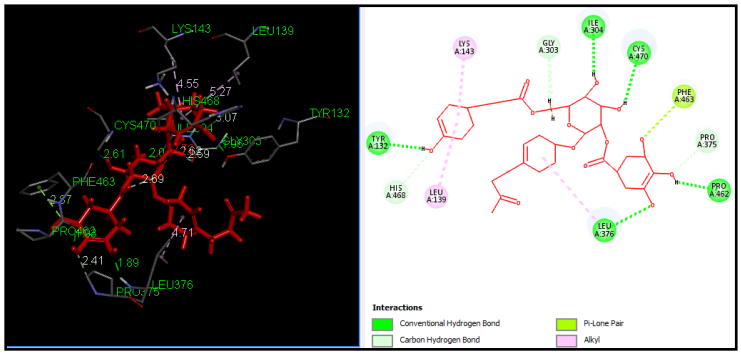

Figure 2: Binding mode of 4-(4-Hydroxyphenyl)-2 butanone O-[2-galloyl-6-pcoumaroylglucoside] at the binding site of sterol 14-alpha demethylase (CYP51) from C. *albicans*

The Phytochemical Catechin 3,5-diglucosideshown with intense network of molecular interactions with binding energy -5.5553Kcal/Mol. Polar amino acid TYR118 interact with hydroxyl group hydrogen atom of terminal glucose unit ring with conventional hydrogen bond interactions with distance of 1.86Å. Positively charged amino acid residues ARG381 interacts with hydroxyl group oxygen atom of glucose unit by forming conventional hydrogen bond interactions with distance of 1.95 and 1.61 Å respectively. Nonpolar amino acid residues PHE463 interacts with hydroxyl hydrogen atom of glucose unit by conventional hydrogen bond interactions with distance of 2.16Å respectively. Nonpolar amino acid PRO462 interacts with hydroxyl group hydrogen of benzopyran scaffold by forming conventional hydrogen bond interactions with distance of 2.20Å. Nonpolar amino acid GLY303 interact with hydrogen atom of hydroxyl group by forming conventional hydrogen bond interactions with distance of 2.21Å. Binding site amino acid residue such as ILE304,PRO375,THR311, CYS470, PRO375 interacts with carbon hydrogen bond interaction Pi donar, Pi-alkyl and alkyl interactions with various distances as shown in figure 3

International Journal of Environmental Sciences
ISSN: 2229-7359
Vol. 11 No. 6s, 2025
https://www.theaspd.com/ijes.php

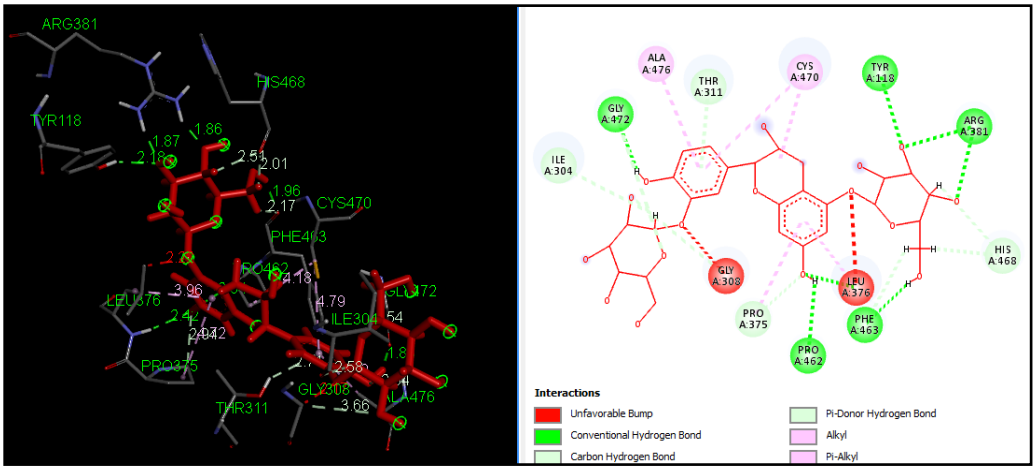

Figure 3: Binding mode of Catechin 3,5-diglucosideat the binding site of sterol 14-alpha demethylase (CYP51) from C. *albicans*

The Phytochemical Paroramine shown with intense network of molecular interactions of conventional hydrogen bond with binding energy -4.6609Kcal/Mol. Polar amino acid TYR132 interact with hydroxyl group hydrogen atom of terminal aglucose unit ring with conventional hydrogen bond interactions with distance of 1.85Å. Positively charged amino acid residues HIS468 interacts with hydrogen atomamino group of aglucose unit by forming conventional hydrogen bond interactions with distance of 2.13Å respectively. Another positively charged amino acid residues ARG469 interacts another hydrogen of amino group of ofaglucose unit by conventional hydrogen bond interactions with distance of 1.94Å respectively. Nonpolar amino acid GLY303 interacts with hydroxyl group hydrogen and amino group hydrogen atom of glucose unit by forming conventional hydrogen bond interactions with distance of 2.03 and 2.70Å respectively. Nonpolar amino acid GLY308 and ILE304 interact with hydrogen atoms of hydroxyl group of glucose unit by forming conventional hydrogen bond interactions with distance of 2.14 and 2.09Å as shown in figure 4

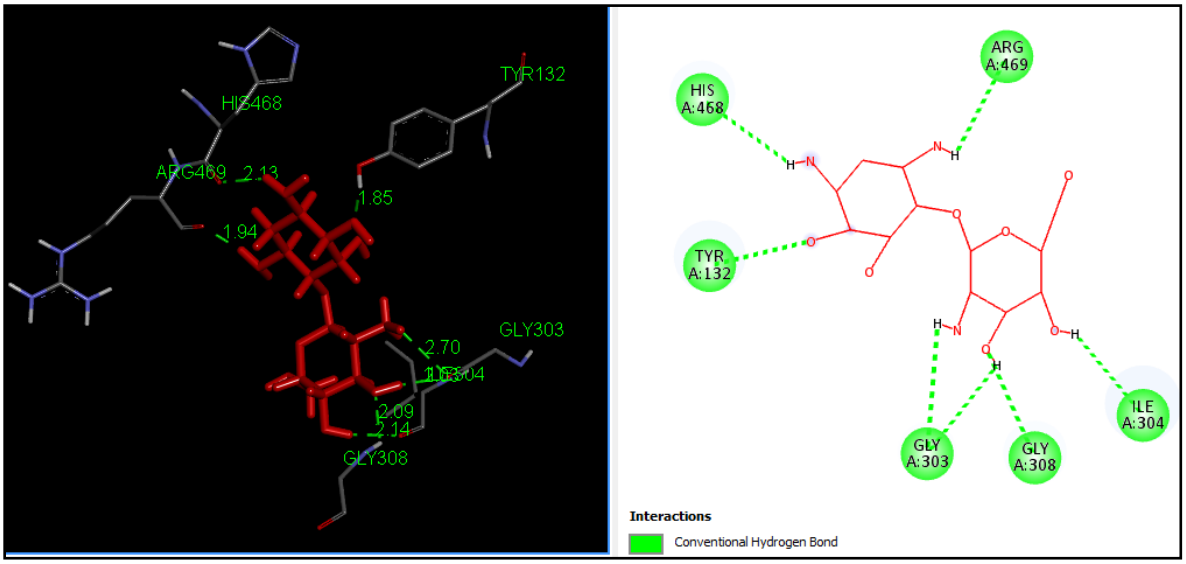

Figure 4: Binding mode of Paroramine at the binding site of sterol 14-alpha demethylase (CYP51) from C. *albicans*

International Journal of Environmental Sciences
ISSN: 2229-7359
Vol. 11 No. 6s, 2025
https://www.theaspd.com/ijes.php

The anti-protease potential of Phytochemical is evaluated by molecular docking studies using the crystal structure of COVID-19 main protease in complex with an inhibitor N3(PDB ID: 6LU7). The molecular docking study suggest that Paromamine, Catechin 3',5-diglucoside and 4-(4-Hydroxyphenyl)-2 butanone O-[2-galloyl-6-pcoumaroylglucoside] have highest inhibitory potential indicated by docking score -7.5971 Kcal/Mol, -3.1349 Kcal/Mol and -2.2395 Kcal/Mol respectively among the all the phytochemicals.

The Phytochemical Paroramine shown with intense network of molecular interactions of conventional hydrogen and carbon hydrogen bond with binding energy -7.5971Kcal/Mol. Polar amino acid THR24 interact with amino group hydrogen atoms of aglucose and glucose unit with conventional hydrogen bond interactions with distance of 1.94 and 2.19Å. Polar amino acids THR25 and THR45 interact with hydrogen atoms amino group of glucose unit by forming conventional hydrogen bond interactions with distance of 2.18 and 1.94Å respectively. Polar amino acid residues SER46 interacts with hydrogen atom of glucose unit by conventional hydrogen bond and carbon hydrogen bond interactions with distance of 2.59,2.23 and 3.06 and Å respectively as shown in figure 5

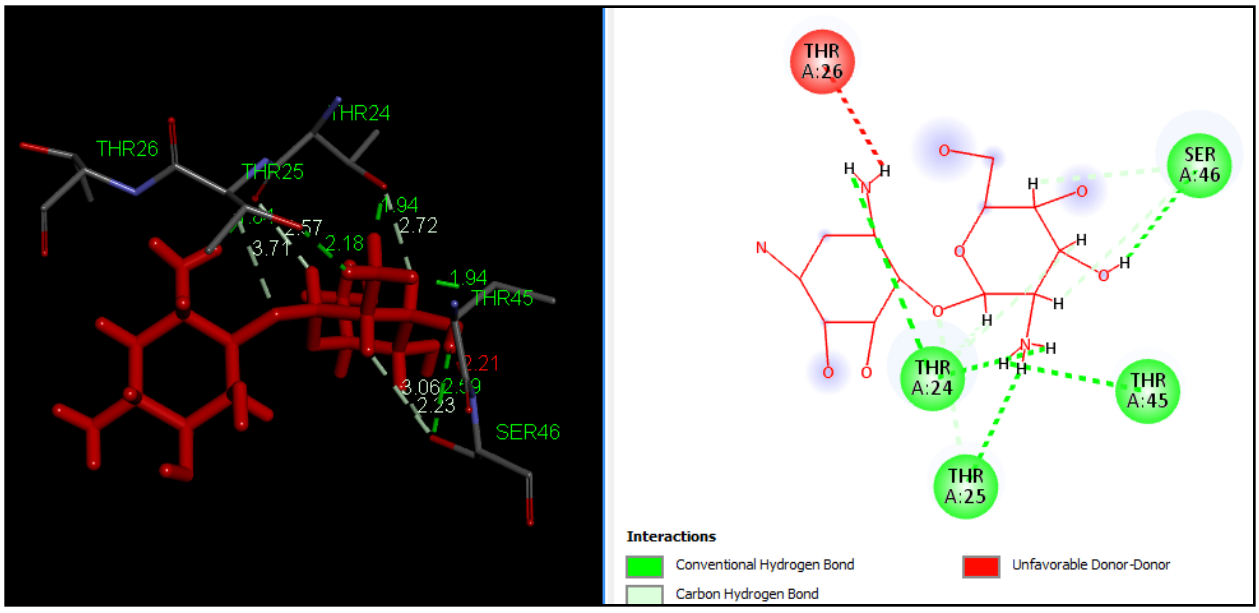

Figure 5: Binding mode of Paroramine at the binding site of main protease of COVID-19

The Phytochemical Catechin 3,5-diglucosideshowsbinding energy -3.1349 Kcal/Mol. Polar amino acid SER46 interact with hydroxyl group hydrogen atom of terminal glucose unit ring with conventional hydrogen bond carbon hydrogen bond interactions with distance of 1.95 and 3.04Å. Polar amino acid residues THR24 interacts with hydroxyl group oxygen atom of glucose unit and oxygen atom of by forming carbon hydrogen bond interactions with distance of 1.24 and 2.40Å respectively. Polar amino acid residues THR25 interacts with ether bridgeoxygen atom of glucose and benzopyran scaffold by carbon hydrogen bond interactions with distance of 3.40Å respectively. Polar amino acid ASN119 interacts with hydroxyl group hydrogen of phenyl ring by forming carbon hydrogen bond interactions with distance of 2.14Å. Anotherpolar amino acid ASN142 interact with hydrogen atom of hydroxyl group of glucose unit by forming carbon hydrogen bond interactions with distance of 2.40Å as shown in figure6

International Journal of Environmental Sciences
ISSN: 2229-7359
Vol. 11 No. 6s, 2025
https://www.theaspd.com/ijes.php

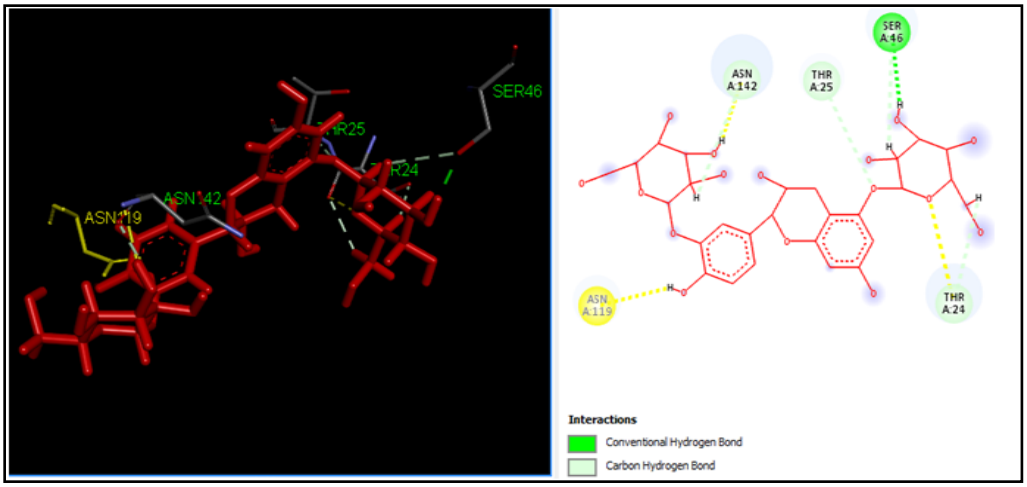

Figure 6: Binding mode of Catechin 3,5-diglucosideat the binding site of main protease of COVID-19

The 4-(4-Hydroxyphenyl)-2 butanone O-[2-galloyl-6-pcoumaroylglucoside]shown binding energy -2.2395 Kcal/Mol. Polar amino acid ASN142 interact with hydroxyl group hydrogen atom of glucose unitoxygen atom of hydroxyl group with conventional hydrogen bond interactions with distance of 3.36Å. Polar amino acid residues THR25 and Nonpolar amino acid CYS44 interact with hydroxyl hydrogenatom of galloyl unit by forming conventional hydrogen bond interactions with distance of 1.97 and 2.04Å respectively. Positively charged amino acid residueHIS41 interacts with galloyl unit hydroxyl hydrogen atoms by conventional hydrogen bond interactions with distance of 1.84 and 1.94Å respectively. Polar amino acid THR24 interacts with hydrogen atom of aglucose side unitwith distance of 2.47 as shown in figure 7

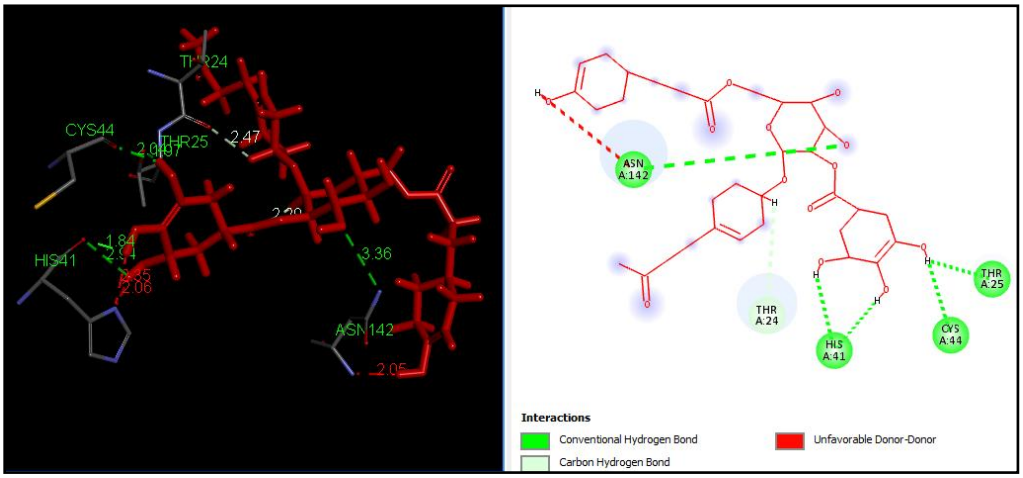

Figure 7: Binding mode of 4-(4-Hydroxyphenyl)-2 butanone O-[2-galloyl-6-pcoumaroylglucoside]at the binding site of main protease of COVID-19

The antibacterial potential of Phytochemical is evaluated against gram negative and gram positive bacterial strains by molecular docking studies using the Crystal Structure of *E.* coli 24kDa Domain in Complex with Clorobiocin (PDB ID: 1KZN) and Crystal Structure of *Staph*ParE 24kDa in complex with Novobiocin(PDB ID: 4URN). The molecular docking study suggest that 4-(4-Hydroxyphenyl)-2 butanone O-[2-galloyl-6-pcoumaroylglucoside], Catechin 3',5-diglucosideand Paromaminehave highest inhibitory potential indicated

International Journal of Environmental Sciences
ISSN: 2229-7359
Vol. 11 No. 6s, 2025
https://www.theaspd.com/ijes.php

by docking score -8.1188Kcal/Mol, -5.5792 Kcal/Mol and -5.4654 Kcal/Mol and-11.704 Kcal/Mol, -7.9564 Kcal/Mol, -7.5505 Kcal/Mol respectivelyamong the all the phytochemicals.

The 4-(4-Hydroxyphenyl)-2 butanone O-[2-galloyl-6-pcoumaroylglucoside]shown high binding energy -8.1138 Kcal/Mol against Crystal Structure of *E.* coli 24kDa Domain in Complex with Clorobiocin (PDB ID: 1KZN). Nonpolar amino acids VAL43 and VAL71 interact with hydroxyl group hydrogen atoms of galloyl ring with conventional hydrogen bond interactions with distance of 2.07 and 2.15Å respectively. Polar amino acid residues THR165 interact with hydroxyl hydrogenof galloyl and ether bridge oxygen atom of galloyl and glucose unit forming conventional hydrogen bond interactions with distance of 1.98 and 2.98Å respectively. Nonpolar amino acid residue GLY77 interacts with aglucose unit oxygen atoms by conventional hydrogen bond interactions with distance of 1.98Å. Nonpolar amino acid ALA86 interact with aglucose unit hydrogen atom of hydroxyl group by forming conventional hydrogen bond interaction1.96Å. Nonpolar amino acid residue VAL120 and Polar amino acid reside SER121 interact with terminal acetyl unit carbonyl oxygen atom by forming conventional hydrogen bond interactions 1.91 and 2.48Å respectively. TheILE78, PRO79, ALA86, ILE90 interacts with alkyl interactions with various distances as shown in figure 8

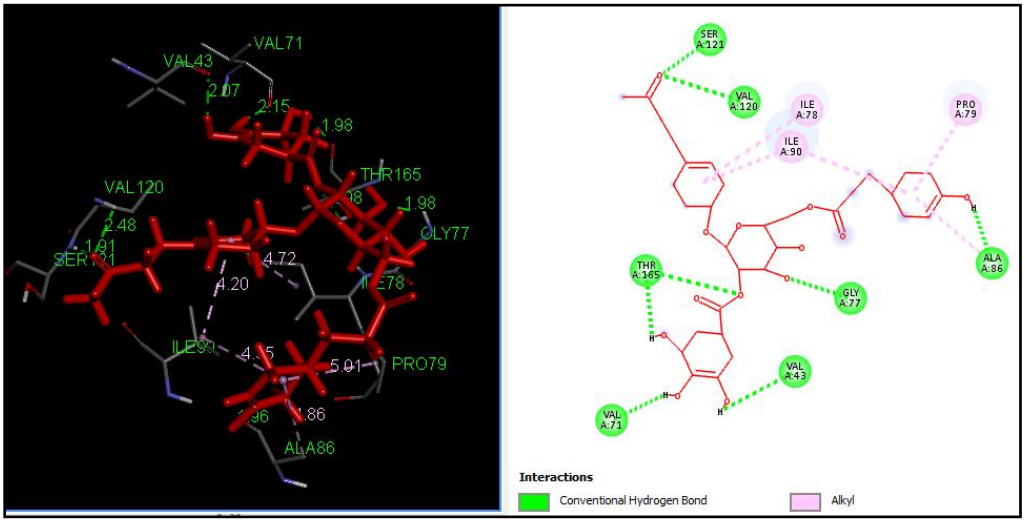

Figure 7: Binding mode of 4-(4-Hydroxyphenyl)-2 butanone O-[2-galloyl-6-pcoumaroylglucoside]at the binding site of Crystal Structure of E. coli

The Phytochemical Catechin 3,5-diglucosideshows binding energy -5.5792Kcal/Mol. Nonpolar amino acid ALA53 interact with hydroxyl group hydrogen atom of terminal glucose unit ring with conventional hydrogen interaction with distance of 2.09Å. Positively charged amino acid ARG76 interacts with oxygen of glucose unit and oxygen atom of hydroxyl group of Benzopyran scaffold by forming conventional carbon hydrogen bond interactions with distance of 2.27 and 2.74Å respectively. Nonpolar amino acid residue GLY77interact hydrogen atom of hydroxyl group of 2.30 Å. Nonpolar amino acid VAL43interact with hydroxyl atom of glucose unit to form conventional hydrogen bond interaction with distance of 1.92Å. Polar amino acid residue THR165 interactswith ether bridge oxygen atom of glucose and benzopyran scaffold and hydrogen atom of glucose unit by forming conventional hydrogen and carbon hydrogen bond interactions with distance of 2.70 and 2.32 and 2.42Å respectively. The amino acid residue GLU50, ILE77, and GLY77 and PRO79 interacts with various distances by forming Pi-Lone, Pi-sigma, alkyl and Pi-alkyl interactions as shown in figure 8

International Journal of Environmental Sciences
ISSN: 2229-7359
Vol. 11 No. 6s, 2025
https://www.theaspd.com/ijes.php

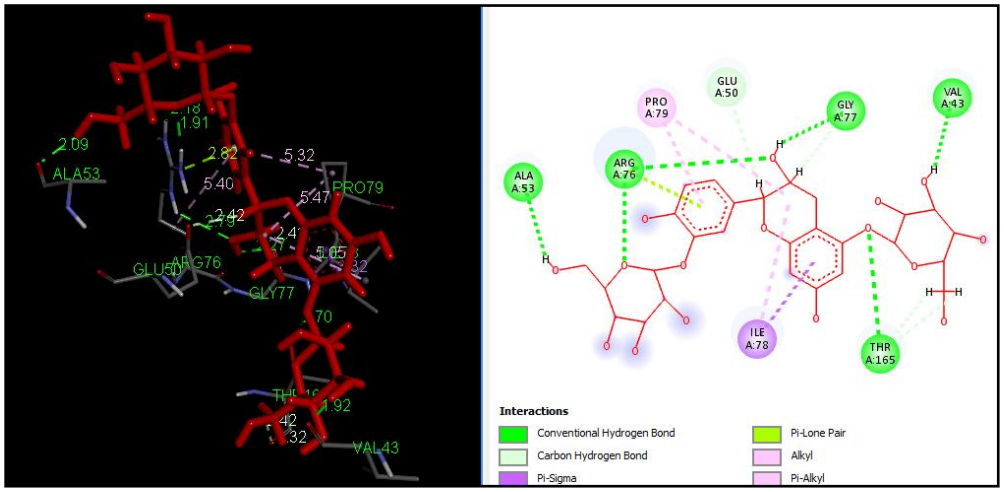

Figure 8: Binding mode of Catechin 3,5-diglucosideat the binding site of Crystal Structure of E. coli

The Phytochemical Paroramine shown with intense network of molecular interactions of conventional hydrogen and carbon hydrogen bond with binding energy -5.4654Kcal/Mol.Negative charged amino acid GLU50interact with amino group hydrogen atoms of glucose unit with conventional hydrogen bond interactions with distance of 3.06 Å. Polar amino acids ASN46 interact with amino group hydrogen atom of glucose and amino group nitrogen of glucose unit by forming convential hydrogen bond interactions with distance of 2.11 and 2.26 Å respectively. and conventionalhydrogen atoms amino group of glucose unit by forming conventional Negatively charged amino acid ASP73 and polar amino acid residue THR165 interacts with oxygen and hydrogen atom of hydroxyl group of aglucose unit by forming conventional carbon hydrogen bond interactions with distance of 3.06 and 2.23Å respectively. Nonpolar amino acid residues VAL43 interacts with hydrogen atom of aglucose unit by forming carbon hydrogen bond interaction with distance of 2.80Å respectively as shown in figure 9

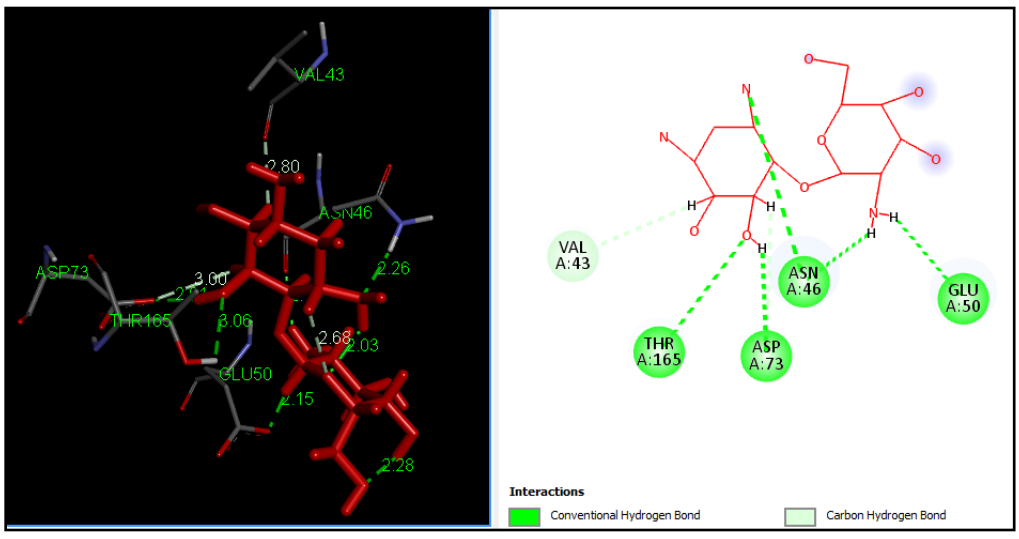

Figure 9: Binding mode of Paroramineat the binding site of Crystal Structure of E. coli

International Journal of Environmental Sciences
ISSN: 2229-7359
Vol. 11 No. 6s, 2025
https://www.theaspd.com/ijes.php

The antioxidant potential of Phytochemical is evaluated by molecular docking studies using the crystal structure of catalase(PDB ID: 2CAG). The molecular docking study suggest that 4-(4-Hydroxyphenyl)-2 butanone O-[2-galloyl-6-pcoumaroylglucoside]Catechin 3',5-diglucoside and Paromamine have highest inhibitory potential indicated by docking score -4.8993Kcal/Mol, -3.4516Kcal/Mol and -3.2878Kcal/Mol respectively among the all the phytochemicals.

The Phytochemical Catechin 3,5-diglucoside shown with intense network of molecular interactions with binding energy -5.4516Kcal/Mol.Positive charged amino acid HIS54 and Nonpolar amino acid residues interact with hydroxyl group hydrogen atom of terminal glucose unit ring with conventional hydrogen bond interactions with distance of 2.71 and 1.92Å respectively. Polar amino acid residueASN144 interacts with hydroxyl group oxygen atom of glucose unit by forming conventional hydrogen bond interactions with distance of 1.94Å. Nonpolar amino acid residueLEU138interacts with hydroxyl hydrogen atom and hydrogen atom of glucose unit by forming conventional hydrogen bond and carbon hydrogen bond interactions with distance of 1.90 and 3.08Å respectively. Negatively charged amino acid ASP142 interacts with hydroxyl group hydrogen of glucose unit by forming conventional hydrogen bond interactions with distance of 1.43 Å. Binding site amino acid residue such as ARG52, PHE140 and PRO141 interacts with carbon hydrogen bond interaction Pi donar, Pi-alkyl and alkyl interactions with various distances as shown in figure 10

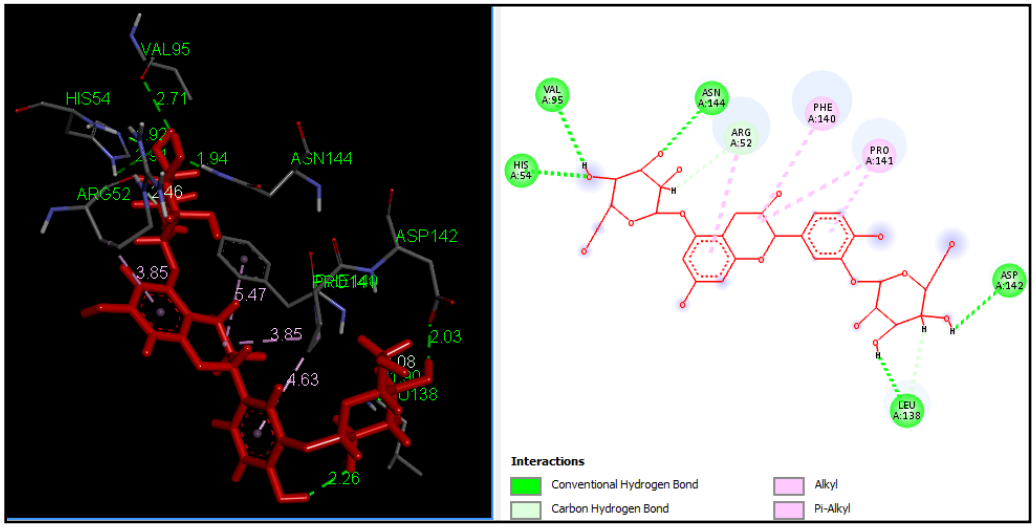

Figure 10: Binding mode of Catechin 3,5-diglucosideat the binding site of Catalase

The 4-(4-Hydroxyphenyl)-2 butanone O-[2-galloyl-6-pcoumaroylglucoside]shown high binding energy -4.8993Kcal/Mol. Positively charged amino acids ARG52 interact with ester linkage carbonyl oxygen atom to form conventional hydrogen bond interactions with distance of 2.58 Å. Nonpolar amino acid residues PRO137 interact with hydroxyl hydrogen of galloyl by forming conventional hydrogen bond interactions with distance of 1.87 Å. Nonpolar amino acid residue TYR343 interacts with aglucose unit Pi electron cloud by forming Pi-alkyl interactions with distance of 5.12 Å. Positively charged amino acid residue ARG52 and Nonpolar amino acid PHE140 interact with aglucose unit forming alkyl and Pi-alkyl interactions with the distance of 4.14 and 4.77 Å respectively as shown in figure 11

International Journal of Environmental Sciences
ISSN: 2229-7359
Vol. 11 No. 6s, 2025
https://www.theaspd.com/ijes.php

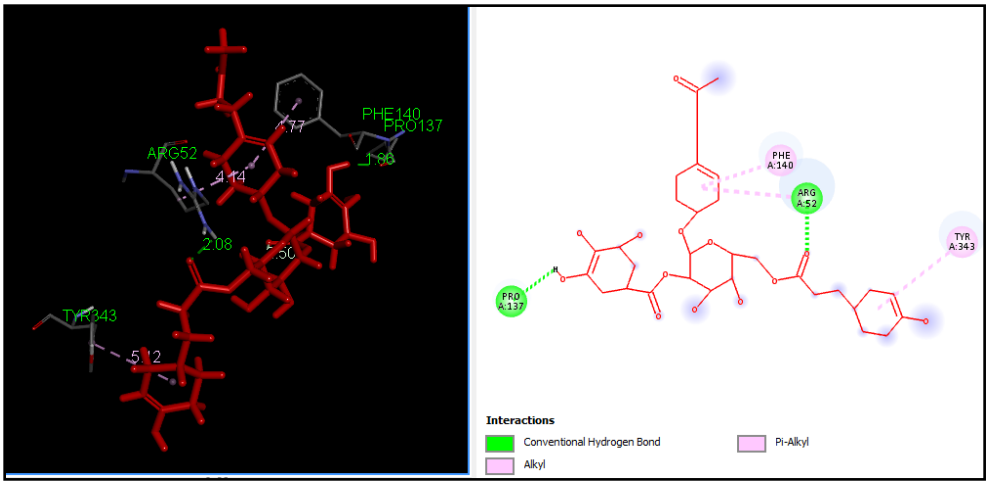

Figure 11: Binding mode of 4-(4-Hydroxyphenyl)-2 butanone O-[2-galloyl-6-pcoumaroylglucoside]at the binding site of Catalase

The Phytochemical Paroramine shown weak network of molecular interactions of binding energy -2.2878Kcal/Mol. positive charged amino acid ARG52 interact with amino group hydrogen atoms of glucose unit with conventional hydrogen bond interactions with distance of 1.76Å. Nonpolar amino acids PHE140 interact with Pi electron cloud of glucose unit by forming Pi-alkyl interaction with distance of 4.79 Å as shown in figure 12

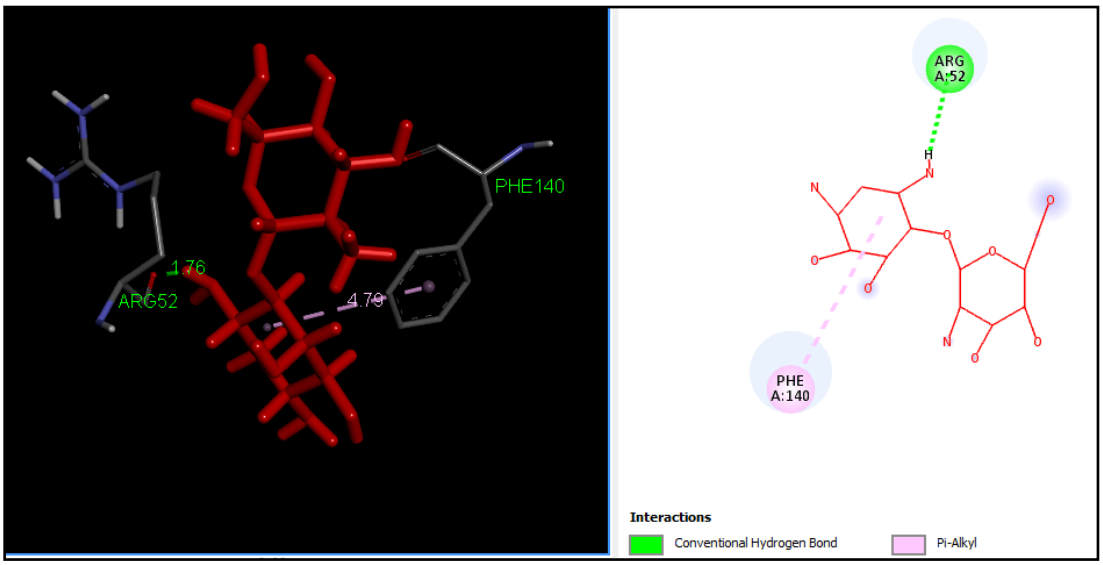

Figure 12: Binding mode of Paroramineat the binding site of Catalase

4. Conclusion:

The current study highlights that the predicted pharmacokinetic and toxicity profile of given phytochemicals extracted from *Avicennia marina* have excellent ADME and no toxicity issues. The oral activity prediction rule of five suggests that most of them follow the permissible limits which highlight their Druglikness. Predicted quantitative property activity relationship models in the study insights relationship of E_{LUMO} and suggesting

it is important for the clearance. The insilico inhibitory. The Molecular docking of Phytochemical suggest that 4-(4-Hydroxyphenyl)-2 butanone O-[2-galloyl-6-pcoumaroylglucoside], Catechin 3',5-diglucoside and Paromamine are the most potent having antifunagal, antiprotease(COVID-19),antibacterial and antioxidant potentials. The mentioned Phytochemicals as they have strong inhibitory potential may act as good leads for the difference cancerous conditions.

REFERENCES:

Agamah, F. E., Mazandu, G. K., Hassan, R., Bope, C. D., Thomford, N. E., Ghansah, A., & Chimusa, E. R. (2020). Computational/in silico methods in drug target and lead prediction. *Briefings in Bioinformatics*, *21*(5), 1663–1675. https://doi.org/10.1093/bib/bbz103

Agu, P. C., Afiukwa, C. A., Orji, O. U., Ezeh, E. M., Ofoke, I. H., Ogbu, C. O., Ugwuja, E. I., & Aja, P. M. (2023). Molecular docking as a tool for the discovery of molecular targets of nutraceuticals in diseases management. *Scientific Reports*, *13*(1), 13398. https://doi.org/10.1038/s41598-023-40160-2

Akolkar, S. V., Nagargoje, A. A., Shaikh, M. H., Warshagha, M. Z. A., Sangshetti, J. N., Damale, M. G., & Shingate, B. B. (2020). New phenylacetamide-linked 1,2,3-triazole-tethered coumarin conjugates: Synthesis, bioevaluation, and molecular docking study. *Archiv Der Pharmazie*, *353*(11), 2000164. https://doi.org/10.1002/ardp.202000164

Allouche, A.-R. (2011). Gabedit—A graphical user interface for computational chemistry softwares. *Journal of Computational Chemistry*, *32*(1), 174–182. https://doi.org/10.1002/jcc.21600

Anwar, S., Alrumaihi, F., Sarwar, T., Babiker, A. Y., Khan, A. A., Prabhu, S. V., & Rahmani, A. H. (2024). Exploring Therapeutic Potential of Catalase: Strategies in Disease Prevention and Management. *Biomolecules*, *14*(6), 697. https://doi.org/10.3390/biom14060697

Arulanandam, C. D., Hwang, J.-S., Rathinam, A. J., & Dahms, H.-U. (2022). Evaluating different web applications to assess the toxicity of plasticizers. *Scientific Reports*, *12*(1), 19684. https://doi.org/10.1038/s41598-022-18327-0

Banerjee, P., Kemmler, E., Dunkel, M., & Preissner, R. (2024). ProTox 3.0: A webserver for the prediction of toxicity of chemicals. *Nucleic Acids Research*, *52*(W1), W513–W520. https://doi.org/10.1093/nar/gkae303

Basyuni, M., Illian, D. N., Istiqomah, M. A., Sari, D. P., Nuryawan, A., Hasibuan, P. A. Z., Sumaiyah, S., & Siregar, E. S. (2019). Prominent Secondary Metabolites from Selected Genus of Avicennia Leaves. *Open Access Macedonian Journal of Medical Sciences*, *7*(22), 3765–3768. https://doi.org/10.3889/oamjms.2019.499

Benet, L. Z., Hosey, C. M., Ursu, O., & Oprea, T. I. (2016). BDDCS, the Rule of 5 and drugability. *Advanced Drug Delivery Reviews*, *101*(1), 89–98. https://doi.org/10.1016/j.addr.2016.05.007

Chaachouay, N., & Zidane, L. (2024). Plant-Derived Natural Products: A Source for Drug Discovery and Development. *Drugs and Drug Candidates*, *3*(1), 184–207. https://doi.org/10.3390/ddc3010011

Collin, F., Karkare, S., & Maxwell, A. (2011). Exploiting bacterial DNA gyrase as a drug target: Current state and perspectives. *Applied Microbiology and Biotechnology*, *92*(3), 479–497. https://doi.org/10.1007/s00253-011-3557-z

De Lile, J. R., Kang, S. G., Son, Y.-A., & Lee, S. G. (2020). Do HOMO–LUMO Energy Levels and Band Gaps Provide Sufficient Understanding of Dye-Sensitizer Activity Trends for Water Purification? *ACS Omega*, *5*(25), 15052–15062. https://doi.org/10.1021/acsomega.0c00870

Doak, B. C., & Kihlberg, J. (2017). Drug discovery beyond the rule of 5—Opportunities and challenges. *Expert Opinion on Drug Discovery*, *12*(2), 115–119. https://doi.org/10.1080/17460441.2017.1264385

ElDohaji, L. M., Hamoda, A. M., Hamdy, R., & Soliman, S. S. M. (2020). Avicennia marina a natural reservoir of phytopharmaceuticals: Curative power and platform of medicines. *Journal of Ethnopharmacology*, *263*(1), 113179. https://doi.org/10.1016/j.jep.2020.113179

Hwang, S. B., Lee, C. J., Lee, S., Ma, S., Kang, Y.-M., Cho, K. H., Kim, S.-Y., Kwon, O. Y., Yoon, C. N., Kang, Y. K., Yoon, J. H., Nam, K.-Y., Kim, S.-G., In, Y., Chai, H. H., Acree, W. E., Grant, J. A., Gibson, K. D., Jhon, M. S., … No, K. T. (2020). PMFF: Development of a Physics-Based Molecular Force Field for Protein Simulation and Ligand Docking. *The Journal of Physical Chemistry B*, *124*(6), 974–989. https://doi.org/10.1021/acs.jpcb.9b10339

Jin, Z., Du, X., Xu, Y., Deng, Y., Liu, M., Zhao, Y., Zhang, B., Li, X., Zhang, L., Peng, C., Duan, Y., Yu, J., Wang, L., Yang, K., Liu, F., Jiang, R., Yang, X., You, T., Liu, X., … Yang, H. (2020). Structure of Mpro from SARS-CoV-2 and discovery of its inhibitors. *Nature*, *582*(7811), 289–293. https://doi.org/10.1038/s41586-020-2223-y

Katritzky, A. R., Kuanar, M., Slavov, S., Hall, C. D., Karelson, M., Kahn, I., & Dobchev, D. A. (2010). Quantitative Correlation of Physical and Chemical Properties with Chemical Structure: Utility for Prediction. *Chemical Reviews*, *110*(10), 5714–5789. https://doi.org/10.1021/cr900238d

Kauthale, S., Tekale, S., Damale, M., Sangshetti, J., & Pawar, R. (2017). Synthesis, antioxidant, antifungal, molecular docking and ADMET studies of some thiazolyl hydrazones. *Bioorganic & Medicinal Chemistry Letters*, *27*(16), 3891–3896. https://doi.org/10.1016/j.bmcl.2017.06.043

Mirazi, N., Movassagh, S.-N., & Rafieian-Kopaei, M. (2016). The protective effect of hydro-alcoholic extract of mangrove (Avicennia marina L.) leaves on kidney injury induced by carbon tetrachloride in male rats. *Journal of Nephropathology*, *5*(4), 118–122. https://doi.org/10.15171/jnp.2016.22

Monk, B. C., Sagatova, A. A., Hosseini, P., Ruma, Y. N., Wilson, R. K., & Keniya, M. V. (2020). Fungal Lanosterol 14α-demethylase: A target for next-generation antifungal design. *Biochimica et Biophysica Acta (BBA) - Proteins and Proteomics*, *1868*(3), 140206. https://doi.org/10.1016/j.bbapap.2019.02.008

Muteeb, G., Rehman, M. T., Shahwan, M., & Aatif, M. (2023). Origin of Antibiotics and Antibiotic Resistance, and Their Impacts on Drug Development: A Narrative Review. *Pharmaceuticals*, *16*(11), 1615. https://doi.org/10.3390/ph16111615

Nainggolan, S. I., Rajuddin, R., Kamarlis, R. K., Hambal, M., & Frengki, F. (2025). In silico study of the potential of curcumin and its derivatives for increasing wild-type p53 expression and improving the function of p53 mutant R273H. *Veterinary World*, *4*(4), 715–730. https://doi.org/10.14202/vetworld.2025.715-730

Naithani, U., & Guleria, V. (2024). Integrative computational approaches for discovery and evaluation of lead compound for drug design. *Frontiers in Drug Discovery*, *4*(103), 1362456. https://doi.org/10.3389/fddsv.2024.1362456

Pires, D. E. V., Blundell, T. L., & Ascher, D. B. (2015). pkCSM: Predicting Small-Molecule Pharmacokinetic and Toxicity Properties Using Graph-Based Signatures. *Journal of Medicinal Chemistry*, *58*(9), 4066–4072. https://doi.org/10.1021/acs.jmedchem.5b00104

Trott, O., & Olson, A. J. (2010). AutoDock Vina: Improving the speed and accuracy of docking with a new scoring function, efficient optimization and multithreading. *Journal of Computational Chemistry*, *31*(2), 455–461. https://doi.org/10.1002/jcc.21334

Van Den Maagdenberg, H. W., Šícho, M., Araripe, D. A., Luukkonen, S., Schoenmaker, L., Jespers, M., Béquignon, O. J. M., González, M. G., Van Den Broek, R. L., Bernatavicius, A., Van Hasselt, J. G. C., Van Der Graaf, Piet. H., & Van Westen, G. J. P. (2024). QSPRpred: A Flexible Open-Source Quantitative Structure-Property Relationship Modelling Tool. *Journal of Cheminformatics*, *16*(1), 128. https://doi.org/10.1186/s13321-024-00908-y

Wu, Z., Shang, X., Liu, G., & Xie, Y. (2023). Comparative analysis of flavonoids, polyphenols and volatiles in roots, stems and leaves of five mangroves. *PeerJ*, *11*, e15529. https://doi.org/10.7717/peerj.15529